Oxidation Behavior of C- and Au-Ion-Implanted Biodegradable Polymers

Emel Sokullu-Urkac, *Member, IEEE*, Ahmet Oztarhan, Funda Tihminlioglu, Alexey Nikolaev, and Ian Brown, *Fellow, IEEE*

***Abstract*—Biodegradable polymers are widely used in biomedical and tissue engineering applications due to their biocompatibility and hydrolysis properties in the body. However, their low surface energy and lack of functional groups to interact with the cellular environment have limited their applications for *in vivo* studies. Ion beam modification is a convenient method for improving the surface properties of polymeric materials for functional biomedical applications. In the work described here, vacuum arc metal ion implantation was used to modify the composition of the near-surface region of three kinds of polymers—poly(L-lactide), poly(D, L-lactide-co-glycolide), and poly(L-lactide/caprolactone)—chosen as representative of biodegradable polymers. X-ray photoelectron spectroscopy analysis was used to characterize the chemical effects of these polymers after implantation with C and with Au, and the results were compared with untreated control samples. We find that oxidation behavior is brought about for certain implantation fluences, resulting in improved surface hydrophilicity.**

***Index Terms*—Biodegradable polymers, ion implantation, surface characterization, X-ray photoelectron spectroscopy (XPS).**

I. Introduction

POLYMER surfaces are of interest as a way of improving the tissue integration of polymeric materials by enhancing tissue cell adhesion to their surfaces. However, improved surface modification procedures are needed to enhance their biocompatibility in a number of aspects. General criteria for selecting a polymer for use as a biomaterial include its mechanical properties (tension, compression, and shear behavior) and the degradation time necessary for the specific application. After fulfilling its purpose, the polymer should degrade at the implantation site, leaving nontoxic residual products. In addition, the surface properties of biomaterials, such as hydrophobicity/hydrophilicity (wettability), surface charge, polarity, and the distribution of reactive chemical groups, may be important issues. Biodegradable polymers offer alternatives for applications in medicine, surgery, etc., and can be either natural or synthetic. Synthetic polymers represent a more reliable source of raw materials, which are important, in turn, for immunogenicity [1]–[4].

Ion beam modification provides a convenient approach for tailoring both the mechanical and chemical properties of polymeric surfaces for biomedical applications [5], [6]. In particular, it has been shown that not only the chemical composition of the irradiated polymer layers can be modified in a controlled way but also the related physical properties can be selectively modified via the ion implantation fluence (in ions per square centimeter).

In the work described here, we have investigated and compared the surface chemistry and wettability of Au^{2+}- and C^{+}-ion-implanted biodegradable polymer samples. The surface carbon dioxide content is a direct indicator of the oxidation level, and higher biodegradability can generally be correlated with higher CO_2 content. Furthermore, ion-catalyzed oxidation of the main polymer chain can lead to an increase in biodegradability [7]–[9]. In the literature, Au has been reported to not only display effective catalytic activity toward the electrochemical behavior of small biomolecules and proteins but also offer a favorable microenvironment for the orientation of several atomic species and greatly facilitate electron transfer [10]. On the other hand, C implantation can generate diamond-like carbon surface properties [11].

The potential ability of carbon and gold ion implantations to alter the cell adhesion properties as well as to modify the material electronic properties and biodegradability are envisaged as part of the oxidative behavior of biodegradable polymers.

II. Experimental Details

A. Materials

Samples of poly-L-lactide (PLA; PURASORB PL18 with an inherent viscosity of 1.8 dL/g), poly-D, L-lactide-co-glycolide 50/50 (PDLG; PURASORB PDLG 5010 with an inherent viscosity of 1.03 dL/g), and poly-L-lactide/caprolactone 70/30 (PLC; PURASORB PLC7015 with an inherent viscosity of 1.63 dL/g) were purchased from PURAC (The Netherlands) in granule form. As a solvent, chloroform (Merck) was used.

B. Film Sample Preparation

PLA, PDLG, and PLC film samples were prepared by a solvent casting method using a 5 wt% polymer–chloroform

Manuscript received July 27, 2011; revised October 24, 2011 and December 6, 2011; accepted December 6, 2011. Date of current version March 9, 2012.

E. Sokullu-Urkac is with BAMM Laboratory, Harvard-MIT Division of Health Sciences and Technology, Cambridge, MA 02139 USA (e-mail: emelsu@gmail.com).

A. Oztarhan is with Ege University, Izmir 35100, Turkey (e-mail: aoztarhan@hotmail.com).

F. Tihminlioglu is with Izmir Institute of Technology, Izmir 35430, Turkey (e-mail: fundatihminlioglu@iyte.edu.tr).

A. Nikolaev is with the Institute of High Current Electronics, Tomsk 634055, Russia (e-mail: nik@opee.hcei.tsc.ru).

I. Brown, retired, was with Lawrence Berkeley National Laboratory, Berkeley, CA 94720 USA. He resides in ... (e-mail: igbrown@lbl.gov).

Color versions of one or more of the figures in this paper are available online at http://ieeexplore.ieee.org.

Digital Object Identifier 10.1109/TPS.2011.2179677

solution. Granules were dissolved in chloroform and prepared by casting of the polymer solution on clean glass slides. The solvent was allowed to evaporate slowly at room temperature for 24 h, and the samples were then dried under vacuum at 50 °C. The films were glossy and with smooth surfaces displaying reproducible contact angle values.

C. Surface Modification

The polymer samples were ion implanted using a vacuum arc ion-source-based ion implantation system at the Ege University Surface Modification Laboratory. This facility has been described in detail elsewhere [12]–[14]. The broad-beam ion source can be repetitively pulsed at rates up to ∼50 pulses/s, and the extracted ion beam current can be up to ∼1 A peak or ∼10 mA time averaged. The ion source extraction voltage can be as high as near 100 kV. Mixed metal/gas ion beams can be generated by adding gas to the arc discharge region. In this paper, carbon and (separately) gold were implanted into polymer-on-glass samples at fluences that were varied over the range of $10^{14}-10^{17}$ ions/cm^2 and at ion energies spanning the range of 20–80 keV.

In order to control the implantation fluence, the number of pulses was varied. The applied pulses and the resulting ion current were measured with an oscilloscope. The fluence was estimated by measuring the implantation current and integrating it over the pulse duration using the following formula:

$$number\ of\ the\ ions\ implanted\ per\ unit\ area\ per\ pulse = \int_{t=0}^{P_w} I \cdot dt/e \cdot \gamma \cdot A$$

where e is the ionic charge, A is the implantation area, I is the ion current, γ is the secondary electron emission coefficient, and P_w is the pulsewidth.

For implantation time t and pulse frequency f, the total fluence is given by

$$fluence = \int_{t=0}^{P_w} I \cdot dt \cdot t \cdot f/e \cdot \gamma \cdot A.$$

The implantation parameters used here were pulse amplitudes which were 20 and 40 kV (extraction voltage) and pulse frequency (f) which was about 0.1–10 Hz.

The SRIM computer code [15], [16] was used to determine the depth profile of the C^+ and Au^{2+} implantations into biodegradable polymeric surfaces. The calculations were performed using a full damage cascade treatment. Parameters were set up to represent the experimental conditions used, i.e., energy of the ions (20–80 keV) and incident angle of 0° (incident ions perpendicular to the substrate) for each polymer. Ion ranges, energy loss distribution of ions, and sputtering yields were recorded after a complete simulation using 99 999 ions.

D. Surface Characterizations

The chemical structure and composition of the implanted surfaces were investigated by X-ray photoelectron spectroscopy (XPS). XPS analysis was carried out using a Thermo K-Alpha monochromatic XPS spectrometer equipped with a dual Al/Mg anode, a hemispherical analyzer, and an electrostatic lens system (Omni Focus III). The electron takeoff angle was 45°, and the analyzer was operated in the FAT mode using the Al K-alpha radiation with pass energies of 100 and 30 eV for survey and high-resolution scans, respectively. The spectra were analyzed using an iterative least squares fitting routine based on Gaussian peaks and Shirley background subtraction.

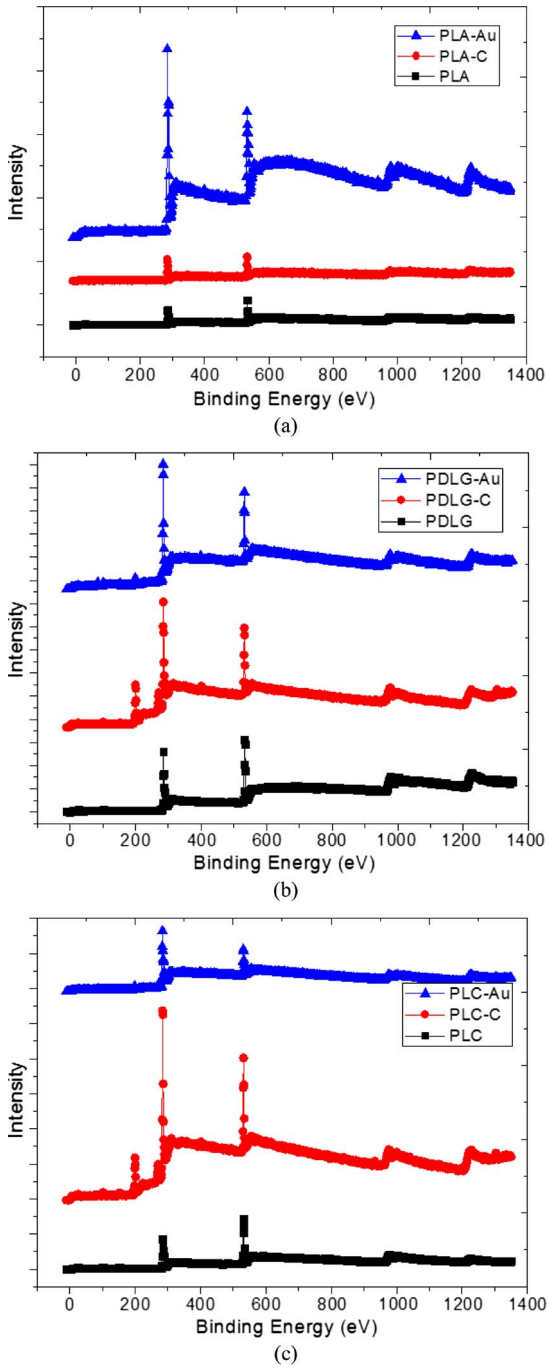

Fig. 1. XPS survey data for implanted polymers: (a) PLA, (b) PDLG, and (c) PLC (implantation parameters are the same). For each polymer, the upper curve is Au implanted (60-keV ion energy and 1×10^{15} ions/cm^2 fluence), the middle curve is C implanted (30-keV ion energy and 1×10^{16} ions/cm^2 fluence), and the lower curve is unimplanted.

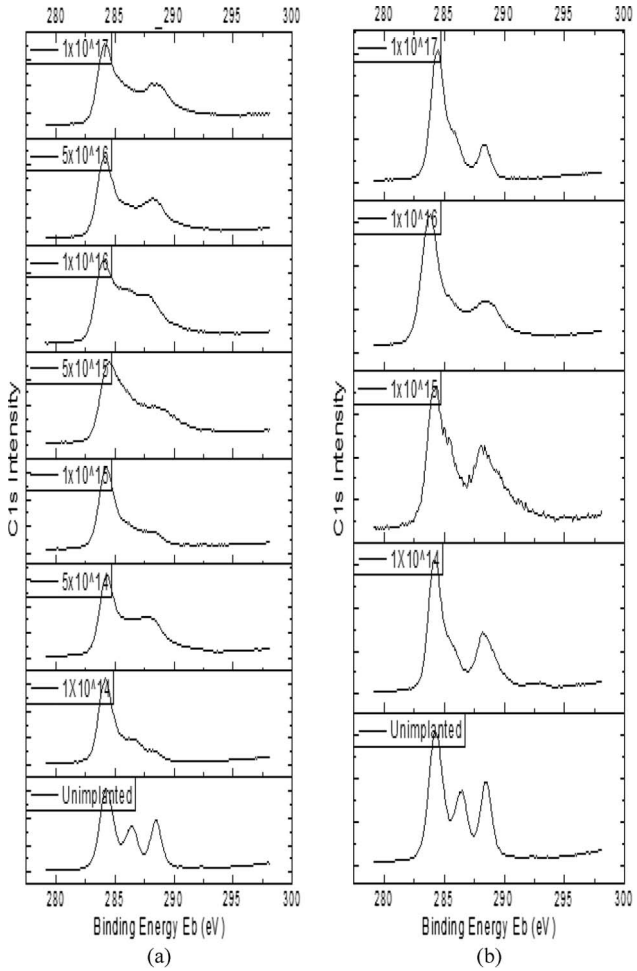

Fig. 2. C 1s intensities of XPS high-resolution data (280–300 eV) for (a) C-implanted PLC and (b) Au-implanted PLC biodegradable polymers as a function of ion fluence. Data for control (unimplanted) samples are also shown.

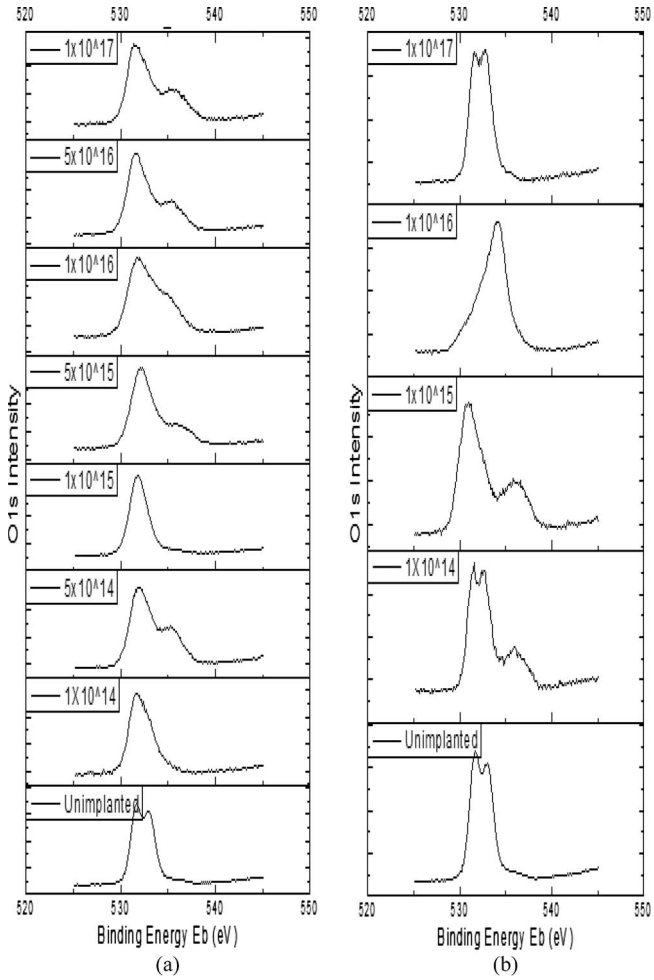

Fig. 3. O 1s intensities of XPS high-resolution data (520–550 eV) for (a) C-implanted PLC and (b) Au-implanted PLC biodegradable polymers as a function of ion fluence. Data for control (unimplanted) samples are also shown.

The chemical shift peaks are charge referenced to the C–C/C–H peak at 284.6 eV.

Contact angles for the determination of the hydrophilic/hydrophobic character of the ion-implanted polymers were estimated from the profile of droplets of distilled water placed on the surface of the material. The contact angle measurements were performed with a Dataphysics OCA-30 system in an atmosphere of air at room temperature. Five different measurements were performed on different areas of the same sample.

III. Results and Discussion

Here, we discuss typical trends in the chemical modification for both Au- and C-implanted polymers as revealed by XPS analysis. The C 1s and O 1s photoelectron peaks of PLA, PDLG, and PLC samples are shown in Fig. 1. The results for different fluences and energies of C and O concentrations can be seen in detail in Figs. 2 and 3, and their structural effects on the $sp2-sp3$ bonding ratio are shown in Table I.

The three different kinds of polymer samples were C and Au implanted, with the same parameters for each kind of polymer, at an ion energy of 60 keV and a fluence of 1×10^{15} ions/cm^2 for the Au implantations and at an ion energy of 30 keV and a fluence of 1×10^{16} ions/cm^2 for the C implantations. In general, the C- and Au-implanted PLA, PLC, and PDLG samples show similar behavior in their XPS characteristics. C–O bonds are broken by the high-energy ion bombardment, and new compounds are formed on the surface. As can be seen in Fig. 1, after implantation, all the samples exhibit increased concentrations of C 1s at 284.9 eV and different behaviors in O 1s around 538.5 eV. The ion implantation simulation results are summarized in Table I, where R_p is the projected range (depth from the surface to the distribution peak) for C^+- and Au^{2+}-ion-implanted poly(L-lactide e-caprolactone) $(C_6H_{10}O_2)_n$, at extraction voltages of 20–40 kV. The tabulated data indicate that the projected ranges for both ion species are of the same order.

TABLE I
SRIM-Calculated Projected Ranges (R_p) of C^+ and Au^{2+} Ions Into PLC Surfaces

C Implanted PLC			Au Implanted PLC		
20 keV	30keV	40keV	40 keV	60keV	80keV
0.2 μm	0.3 μm	0.4 μm	0.08 μm	0.1 μm	0.1 μm

Fig. 2 shows the XPS spectral data for high-resolution C 1s scans. The first component, centered at 285 eV, is attributed to

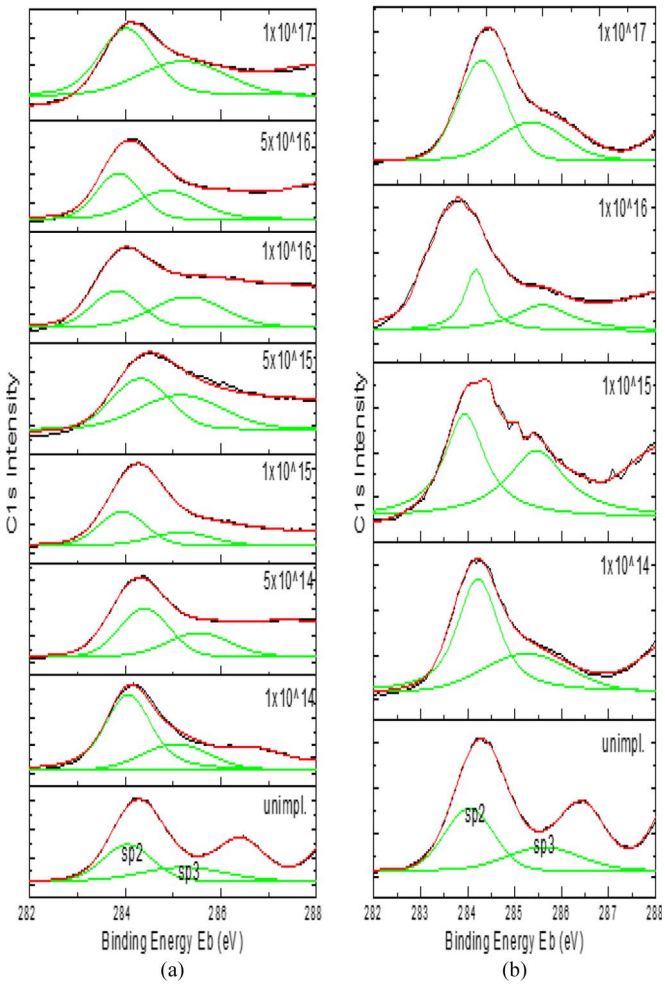

Fig. 4. $sp2$ and $sp3$ hybridizations extracted from C $1s$ spectra for (a) C-implanted PLC and (b) Au-implanted PLC.

aliphatic carbon bonds (–C–C–) and carbon–hydrogen bonds (–C–H–). The second component at 287 eV is attributed to ether bonds (–C–O–), and the third component at 289 eV is assigned to the carboxylic groups (–COOH) in PLC [17], [18].

A decomposition of C $1s$ spectra into two bands provides the average binding energy and width of the corresponding $sp2$ and $sp3$ hybridizations (Fig. 4). A third band at higher binding energy is due to oxidized carbon atoms [19]–[21]. After ion implantation of both C^+ and Au^{2+} into PLC, the C $1s$ spectra are characterized by a single peak; however, the vibrational states for each of the primary lines are responsible for the observed spectrum (Fig. 2). Thus, the peak model requires suitable asymmetric line shapes to describe the vibrational asymmetry (Fig. 4). The vibrational structure is a part of the photon energy absorbed in ways other than purely ejecting an electron from the surface [22]. Other absorption modes, which include the so-called shake-up peaks, are possible where the loss structures appear at lower energy than the primary peaks with magnitude larger than the vibrational energy losses observed in PLC.

Our analysis shows that the $sp3$ band is always broader than the $sp2$ component after ion implantation. As shown in Table II, $sp3$ carbon bonding is equal to or dominant to $sp2$ bonds for C implantation at fluences of 1×10^{15}–1×10^{16} ions/cm^2 and for Au implantation at 1×10^{15} ions/cm^2. This behavior can be correlated with the O $1s$ spectra shown in Fig. 3, which show increased concentration of oxygen for this specific range for the C and Au implantations. Thus, the O $1s$ spectra (Fig. 3) decrease with fluence, and the surface chemical structure of the biodegradable polymer changes back to a graphitic structure (Table II).

TABLE II
FRACTION OF $sp3$-BONDED CARBON IN C-IMPLANTED PLC AND Au-IMPLANTED PLC AS A FUNCTION OF IMPLANTATION FLUENCE

Fluence (ion/cm^2)	sp3/(sp2+sp3)	
	C implanted PLC	Au implanted PLC
Unimplanted	0.4	0.4
1 x 10^{14}	0.3	0.3
5 x 10^{14}	0.4	-
1 x 10^{15}	0.3	0.5
5 x 10^{15}	0.6	-
1 x 10^{16}	0.5	0.5
5 x 10^{16}	0.4	-
1 x 10^{17}	0.4	0.3

Fig. 3 shows the XPS results for high-resolution O $1s$ scans, where the C=O and C–O bonds at 536.0 and 533.4 eV, respectively, can be seen [17], [18]. The O $1s$ spectra in Fig. 3 associate with the C $1s$ spectra in Fig. 2, at the indicated fluence.

In both Figs. 2 and 3, the lower fluence data show a decline in the oxidized vibrational density, a consequence of phenyl rings broken by ion beam bombardment. In this situation, ion-implanted and air-exposed samples are oxidized. As a result, the vibrations mainly exhibited are related to a hydrogenated amorphous carbon phase, which confirms the formation of oxidized carbon compounds including partially degraded aromatic rings [21]–[23]. This behavior is a consequence of atmospheric air in contact with surface open bonds. This situation is evident not only for the C-implanted samples but also for the Au-implanted samples.

In the case of Au implantation, ion bombardment induces carbon depletion from the surface layer, particularly for fluences of 1×10^{15}–1×10^{16} ions/cm^2. The C-implanted samples exhibit the same trend for fluences of 1×10^{16} and 5×10^{16} ions/cm^2.

As can be seen from Fig. 5 and Table III, the oxygen concentration of the untreated sample is 44% and decreases to 22% after C implantation at a fluence of 1×10^{14} ions/cm^2. In the same way as for the Au-implanted material, the decrease in concentration follows the same trend, and the C concentration increases for low-fluence implantation. On the other hand, for fluences of 1×10^{15} and 5×10^{15} ions/cm^2, the reverse behavior is observed. For these fluences for C-implanted samples, the O concentration increases. For 5×10^{16} and 1×10^{17} higher fluences, C and O concentrations on the surface exhibit the same behavior as for low fluences. In general, the C concentration increases, and the O concentration shows a decrease.

Thus, we can say that, for both C and Au implantations at "intermediate" implantation fluence, the surface oxygenation

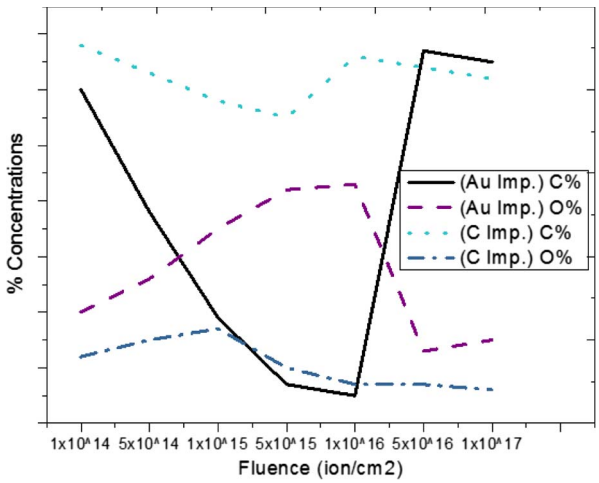

Fig. 5. Surface atomic composition (in terms of concentrations %C and %O) of C-implanted PLC and Au-implanted PLC.

TABLE III
PLC SURFACE ATOMIC COMPOSITION (IN TERMS OF CONCENTRATIONS %C AND %O) OF C AND Au IMPLANTATION FLUENCES

Fluence (ion/cm^2)	Au Implanted PLC			C Implanted PLC		
	C%	O%	Others	C%	O%	Others
Control	**52**	**44**	**4% Si**	**52**	**44**	**4% Si**
1x10^{14}	70	30	-	78	22	-
5x10^{14}	48	36	8% Si 7% N	73	25	2% N
1x10^{15}	29	45	15% Si 11% N	68	27	4% Si 2% N
5x10^{15}	17	52	16% Si 15% N	65	20	11% Cl 2% N 2% Si
1x10^{16}	15	53	17% Si 15% N	76	17	4% Cl 1% Si 2% N
5x10^{16}	77	23	-	74	17	3% Cl 2% N 2% Si
1x10^{17}	75	25	-	72	16	9% Cl 3% Si

increases. This might be the origin of the associated changes in surface reactions and surface energy in terms of surface charge distribution.

It has been reported [28] that the oxidation rate of ion-implanted silicon increases with fluence of Ar^+ and F^+ ions, whereas the implantation energy and, hence, the penetration depth do not have much effect on the silicon oxidation rate, and that the thickness uniformity of the oxide film grown over the surface also improves with increasing implantation fluence. In the present study, the same situation is true for polymers but over a certain fluence range. We also observe improvement in uniformity of the oxidizing species. Defects generated by implantation surpass the existing defects on the film, and the oxidation process is dominated by implantation-generated defects. In such a situation, nonuniformity of the implantation process governs the uniformity of oxidation [19], [21], [28]. The implanted surface also enhances the migration of

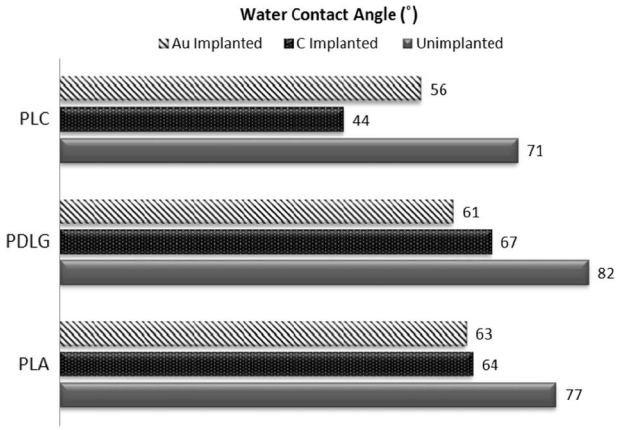

Fig. 6. Mean contact angles for unimplanted and C-implanted and Au-implanted PLA, PDLG, and PLC biodegradable polymers (ion energy of 30 keV and fluence of 5×10^{15} ions/cm^2, for both C and Au implantations).

oxidizing species in polymers, and multidimensional migration of the oxidizers overcomes the enhancement of oxidation sites [28]. The C and O concentrations change with fluence in PLC. Figs. 1–3 suggest that this phenomenon can be extended to different polymeric samples with several ions for lower fluence, but after a threshold value, this behavior tends to decline and the surface becomes carbonized.

It has been reported in the literature [20] that the formation of oxygen functionalities by ion implantation is one of the most useful and effective surface modification processes. Generally, polymers are hydrophobic, and conversion of these polymers from hydrophobic to hydrophilic behavior usually improves the adhesion strength, biocompatibility, and other important properties in physiological conditions and has been directly linked to oxygenation of the surface. In general, increase of carboxyl and C–O–C groups affects the surface energy and tends to improve surface wettability [25]–[28].

Fig. 6 shows the measured water contact angles on PLA, PLC, and PDLG before and after C implantation at a fluence of 5×10^{15} ions/cm^2 and an ion energy of 30 keV. Note that significant surface oxidation is observed by XPS (Figs. 3 and 5 and Table II). All three biodegradable polymers exhibit similarly improved wettability properties.

It can be seen from Fig. 6 that, for all three polymers, the contact angle falls significantly subsequent to both Au and C implantations. This change in water wettability is greatest for C-implanted PLC, for which the 71° unimplanted contact angle decreases to 44° after implantation. Aromatic rings of these polymers interact with polar water molecules through π electrons. After both Au and C implantations, hydrogen bonding and dipole interactions between water molecules and oxygen functional groups on the surface result in improved wettability of all biodegradable polymers [19]–[28].

The overall results indicate that the implanted ions initially cause the destruction of rings of PLC which are composed of aliphatic–aromatic polyesters and the formation of structural defects in the macromolecules. Thus, the processes of structure transformation include degradation of aromatic rings, which are the least stable structures in the polymeric molecules, and this is followed by degradation of aliphatic groups, which are

more stable. As the fluence increases, carbonization processes continue until a dense carbon layer is formed. Fig. 5 and Table III show the oxidation of PLC which occurs from broken component macromolecules of the samples removed from vacuum after intermediate fluences when the damage is high but the density of damage is not yet high enough to result in cross-linking [29].

For these intermediate fluence values, polymeric structure will contain many reactive centers and will readily react with atmospheric oxygen. Again, both Fig. 5 and Table III also confirm that continued ion irradiation induces cross-linking and the formation of a hard amorphous carbon network which does not react with oxygen on exposure to the atmosphere. Therefore, the oxygen concentration has fallen again, and the relative $sp2$ content is also dominant on the surface (Table II).

The formation of amorphous tracks and increasing $sp2$ content are two of the consequences of the ion-induced thermal spike [30]. Possibly, the $sp3$ fraction and the O concentration are highest at intermediate fluence but low at either low or high fluences.

We speculate that this behavior may be due to sputtering, which is explained by a thermal activation mechanism in the literature [30], [31]. Szenes [33]–[35] assumes that the atoms are sputtered mainly from the hottest region. After charge neutralization is completed in the solid, the dominant fraction of the deposited energy is in the electron system. During the relaxation process, this energy is transferred to lattice atoms, leading to the formation of a high-temperature region called the thermal spike. The damage is more severe, and the electron deficit is the highest there. The bonds become temporarily weaker, and high transient mechanical stress field and strong Coulomb forces appear [30], [31]. This results in amorphous tracks on the surfaces.

There are two thermal spike models that are often applied in analysis of the interaction of swift heavy ions with solids: the inelastic thermal spike model (ITSM) [31] and the analytical thermal spike model (ATSM) [32]. The ITSM follows the formation of the ion-induced thermal spike based on the Fourier equation, while the ATSM skips this stage and a final Gaussian temperature distribution is assumed. The ITSM rejects the Gaussian temperature distribution, while according to ATSM, several thermophysical parameters used by the ITSM are irrelevant to the formation of the thermal spike and the equilibrium values are not valid under spike conditions [32]. The results in Fig. 5 and Table III lead us to the ATSM [33]–[36] approach as applicable to the sputtering of PLC molecules as well.

IV. Conclusion

We have shown that ion implantation of C and Au into biodegradable polymers, over a range of implantation fluences, modifies the polymer surface to produce oxygen-containing more hydrophilic surfaces. Surfaces implanted at low and high fluences show the formation of less oxygen groups, while at intermediate implantation fluence, enhanced oxygenation is observed, possibly due to migration of species along chains and atmospheric effects. These results suggest that ion implantation at optimum fluence affects the behavior of biodegradable polymeric materials in highly oxidative environments.

Acknowledgment

The authors would like to thank their colleagues at the Bilkent University National Nanotechnology Research Center (UNAM) for the use of X-ray photoelectron spectroscopy measurement facilities.

References

[1] L. S. Nair and C. T. Laurencin, "Biodegradable polymers as biomaterials," *Progr. Polym. Sci.*, vol. 32, no. 8/9, pp. 762–798, Aug./Sep. 2007.

[2] R. Langer, L. G. Cima, J. A. Tamada, and E. Wintermantel, "Future directions in biomaterials," *Biomaterials*, vol. 11, no. 9, pp. 738–745, Nov. 1990.

[3] M. Vert, "Polymeric biomaterials: Strategies of the past vs. strategies of the future," *Progr. Polym. Sci.*, vol. 32, no. 8/9, pp. 755–761, Aug./Sep. 2007.

[4] L. G. Griffith, "Polymeric biomaterials," *Acta Mater.*, vol. 48, no. 1, pp. 263–277, Jan. 2000.

[5] P. K. Chu, J. Y. Chen, L. P. Wang, and N. Huang, "Plasma-surface modification of biomaterials," *Mater. Sci. Eng. R. Rep.*, vol. 36, no. 5/6, pp. 143–206, Mar. 2002.

[6] E. Sokullu-Urkac, A. Oztarhan, F. Tihminlioglu, N. Kaya, D. Ila, C. Muntele, S. Budak, E. Oks, A. Nikolaev, A. Ezdesir, and Z. Tek, "Thermal characterization of Ag and Ag + N ion implanted ultra-high molecular weight polyethylene (UHMWPE)," *Nucl. Instrum. Methods Phys. Res. B, Beam Interact. Mater. At.*, vol. 261, no. 1/2, pp. 699–703, Aug. 2007.

[7] A. Atala, R. Lanza, J. A. Thomson, and R. M. Nerem, *Principles of Regenerative Medicine*. Amsterdam, The Netherlands: Elsevier, 2008, p. 344.

[8] Y. Tokiwa, B. P. Calabia, C. U. Ugwu, and S. Aiba, "Biodegradability of plastics," *Int. J. Mol. Sci.*, vol. 10, no. 9, pp. 3722–3742, Aug. 2009.

[9] R. W. Lenz, *Advances in Polymer Science*, vol. 107. Berlin, Germany: Springer- Verlag, 1993, pp. 1–40.

[10] C. Liu, Q. Chen, J. Jiao, S. Li, J. Hu, and Q. Li, "Surface modification of indium tin oxide films with Au ions implantation: Characterization and application in bioelectrochemistry," *Surf. Coat. Technol.*, vol. 205, no. 12, pp. 3639–3643, Mar. 2011.

[11] I. G. Brown, A. Anders, M. R. Dickinson, R. A. MacGill, and O. R. Monteiro, "Recent advances in surface processing with metal plasma and ion beams," *Surf. Coat. Technol.*, vol. 112, no. 1–3, pp. 271–277, 1999.

[12] A. Oztarhan, I. Brown, C. Bakkaloglu, G. Watt, P. Evans, E. Oks, A. Nikolaev, and Z. Tek, "Metal vapour vacuum arc ion implantation facility in Turkey," *Surf. Coat. Technol.*, vol. 196, no. 1–3, pp. 327–332, Jun. 2005.

[13] I. G. Brown and X. Godechot, "Vacuum arc ion charge-state distributions," *IEEE Trans. Plasma Sci.*, vol. 19, no. 5, pp. 713–717, Oct. 1991.

[14] I. Gushenets, A. G. Nikolaev, E. M. Oks, L. G. Vintizenko, G. Y. Yushkov, A. Oztarhan, and I. G. Brown, "Simple and inexpensive time-of-flight charge-to-mass analyzer for ion beam source characterization," *Rev. Sci. Instrum.*, vol. 77, no. 6, p. 063 301, Jun. 2006.

[15] J. P. Biersack and L. Haggmark, "A Monte Carlo computer program for the transport of energetic ions in amorphous targets," *Nucl. Instrum. Method*, vol. 174, no. 1/2, pp. 257–269, Aug. 1980.

[16] J. F. Ziegler, *The Stopping and Range of Ions in Matter*, vol. 2–6. New York: Pergamon, 1977–1985.

[17] I. Djordjevic, L. G. Britcher, and S. Kumar, "Morphological and surface compositional changes in poly(lactide-co-glycolide) tissue engineering scaffolds upon radio frequency glow discharge plasma treatment," *Appl. Surf. Sci.*, vol. 254, no. 7, pp. 1929–1935, Jan. 2008.

[18] Y. Wan, X. Qu, J. Lu, C. Zhu, L. Wan, J. Yang, J. Bei, and S. Wang, "Characterization of surface property of poly(lactide-co-glycolide) after oxygen plasma treatment," *Biomaterials*, vol. 25, no. 19, pp. 4777–4783, Aug. 2004.

[19] N. Vandencasteele and F. Reniers, "Plasma-modified polymer surfaces: Characterization using XPS," *J. Electron. Spectrosc.*, vol. 178/179, pp. 394–408, May 2010.

[20] G. Marletta, *Materials Science With Ion Beams*, vol. 116, *Topics in Applied Physics*. Berlin, Germany: Springer-Verlag, 2010, p. 345.

[21] G. Marletta, G. Ciapetti, C. Satriano, S. Pagani, and N. Baldini, "The effect of irradiation modification and RGD sequence adsorption on the response of human osteoblasts to polycaprolactone," *Biomaterials*, vol. 26, no. 23, pp. 4793–4804, Aug. 2005.
[22] G. Beamson and D. Briggs, The XPS of Polymers Database, 2000.
[23] G. Marletta, G. Ciapetti, C. Satriano, F. Perut, M. Salerno, and N. Baldini, "Improved osteogenic differentiation of human marrow stromal cells cultured on ion-induced chemically structured poly-ϵ-caprolactone," *Biomaterials*, vol. 28, no. 6, pp. 1132–1140, Feb. 2007.
[24] I. Amato, G. Ciapetti, S. Pagani, G. Marletta, C. Satriano, N. Baldini, and D. Granchi, "Expression of cell adhesion receptors in human osteoblasts cultured on biofunctionalized poly-(ϵ-caprolactone) surfaces," *Biomaterials*, vol. 28, no. 25, pp. 3668–3678, Sep. 2007.
[25] C. Satriano, G. Marletta, S. Guglielmino, and S. Carnazza, *Contact Angle, Wettability and Adhesion*, vol. 4. Utrecht, The Netherlands: VSP, 2006, pp. 1–16.
[26] C. Satriano, S. Carnazza, S. Guglielmino, and G. Marletta, "Differential cultured fibroblast behavior on plasma and ion-beam-modified polysiloxane surfaces," *Langmuir*, vol. 18, no. 24, pp. 9469–9475, Oct. 2002.
[27] A. Zebda, H. Sabbah, S. Ababou-Girard, F. Solal, and C. Godet, "Surface energy and hybridization studies of amorphous carbon surfaces," *Appl. Surf. Sci.*, vol. 254, no. 16, pp. 4980–4991, Jun. 2008.
[28] R. Kumar, M. S. Yadav, K. Kishore, K. Sambhawam, S. Goyal, D. N. Singh, and P. J. George, "Impact of dose and energy of argon ($^{40}Ar^{+}$) and fluorine ($^{19}F^{+}$) ion implantation on uniformity of silicon oxidation ," *Vacuum*, vol. 81, no. 3, pp. 260–264, Oct. 2006.
[29] B. K. Gan, M. M. M. Bilek, A. Kondyurin, K. Mizuno, and D. R. McKenzie, "Etching and structural changes in nitrogen plasma immersion ion implanted polystyrene films," *Nucl. Instrum. Methods Phys. Res. B, Beam Interact. Mater. At.*, vol. 247, no. 2, pp. 254–260, Jun. 2006.
[30] M. Toulemonde, W. Assmann, C. Dufour, A. Meftah, F. Studer, and C. Trautmann, "Experimental phenomena and thermal spike model description of ion tracks in amorphisable inorganic insulators," *Mat. Fys. Medd. Kong. Dan. Vid. Selsk.*, vol. 52, p. 263, 2006.
[31] G. Szenes, "General features of latent track formation in magnetic insulators irradiated with swift heavy ions," *Phys. Rev. B*, vol. 51, no. 13, pp. 8026–8029, Apr. 1995.
[32] A. Meftah, F. Brisard, J. M. Costantini, E. Dooryhee, M. Hage-Ali, M. Hervieu, J. P. Stoquert, F. Studer, and M. Toulemonde, "Track formation in SiO_2 quartz and the thermal-spike mechanism," *Phys. Rev. B*, vol. 49, no. 18, pp. 12 457–12 463, May 1994.
[33] G. Szenes, "Temperature distribution in a swift ion-induced spike: An experimental approach," *Radiat. Eff. Def. Sol.*, vol. 162, no. 7–8, p. 557, 2007.
[34] G. Szenes, "Scaling law for the ion-induced electronic sputtering of intact biomolecules: Evidence of thermal activation," *Phys. Rev. B*, vol. 70, no. 9, pp. 094 106-1–094 106-6, Sep. 2004.
[35] G. Szenes, "Analysis of the desorption of clusters of intact amino acid valine molecules induced by energetic monoatomic and cluster ions," *Nucl. Instrum. Methods Phys. Res. B, Beam Interact. Mater. At.*, vol. 230, no. 1–4, pp. 502–506, Apr. 2005.
[36] G. Szenes, "Universal scaling for biomolecule desorption induced by swift heavy ions," *Nucl. Instrum. Methods Phys. Res. B, Beam Interact. Mater. At.*, vol. 233, no. 1–4, pp. 70–77, May 2005.

Emel Sokullu-Urkac (M'08) received the B.Sc. degree in physics engineering from Istanbul Technical University, Istanbul, Turkey, the M.Sc. degree in materials science and engineering from Izmir Institute of Technology, Izmir, Turkey, and the Ph.D. degree in bioengineering from Ege University, Izmir.

She is currently a Postdoctoral Research Fellow with BAMM Laboratory, Harvard–MIT Division of Health Sciences and Technology, Cambridge, MA. Her research topic is "ion beam surface modification of polymeric materials for neural applications."

Dr. Sokullu-Urkac is a member of the Biomaterials Network, the European Technology Platform for Advanced Engineering Materials and Technologies, and the Materials Research Society.

Ahmet Oztarhan received the B.S. degree from the Physics Department, Middle East Technical University, Ankara, Turkey, and the Ph.D. degree in plasma physics from the University of Manchester Institute of Science and Technology, Manchester, U.K., in 1982.

For 19 years, he was with the Department of Mechanical Engineering, Dokuz Eylul University, Izmir, Turkey (obtained his professorship in 1993). He has done many projects in Turkey related to surface modification of materials by plasma-based technologies and their industrial applications. Since 2003, he has been with the Bioengineering Department, Ege University, Izmir.

Dr. Oztarhan is a member of the Materials Research Society and the International Scientific Committee of "Surface Modification of Materials by Ion Beams." He was a recipient of a grant from the Turkish Ministry of Education during his Ph.D. study in plasma physics.

Funda Tihminlioglu received the B.S. and M.Sc. degrees from the Chemical Engineering Department, Ege University, Izmir, Turkey, and the Ph.D. degree in chemical engineering from Pennsylvania State University, University Park.

Since 2009, she has been a Professor of chemical engineering with Izmir Institute of Technology, Izmir, Turkey, where she is currently the Dean of the Faculty of Engineering. She is the author and coauthor of more than 40 research papers. Her research interests include polymer processing and characterization, specifically focused on biodegradable polymers and nanocomposites for packaging and biomedical applications.

Prof. Tihminlioglu is a member of the Turkish Chamber of Chemical Engineering.

Alexey Nikolaev received the B.Sc. degree in electronics from Tomsk State University of Control Systems and Radioelectronics, Tomsk, Russia, in 1990 and the Ph.D. degree in vacuum and plasma electronics from the Institute of High Current Electronics, Tomsk, in 1998.

He is currently a Senior Researcher with the Plasma Sources Laboratory, Institute of High Current Electronics, Tomsk, Russia. His scientific activities include investigation of vacuum arc and glow discharge physics, development of charged particle sources for the purpose of charged particle injection in accelerators, and surface modification in different materials, including organic and textile materials.

Ian Brown (F'96) received the Ph.D. degree in plasma physics from The University of Sydney, Sydney, Australia.

He was a Senior Physicist with the Lawrence Berkeley National Laboratory, Berkeley, CA, where, in 1984, he established the Plasma Applications Group and was the Group Leader there until his retirement in February 2001. He has held research and teaching positions at The University of Sydney, Princeton University, Princeton, NJ, the University of California, Berkeley, and the Max-Planck Institute for Plasma Physics, Garching, Germany. He is the author or coauthor of more than 400 research papers, and his book "The Physics and Technology of Ion Sources" (Wiley, 1989 and 2004) has become a standard in the field. His research interests include plasma and ion sources, their applications for materials synthesis and modification, and novel biological applications of plasma and ion beam physics.

Dr. Brown is a Fellow of the American Physical Society, the Institute of Physics (U.K.), and the Australian Institute of Physics. His research has been recognized by three R&D 100 Awards.